University of Groningen

Polarized sphingolipid transport from the subapical compartment

van Ijzendoorn, SCD; Hoekstra, D

IMPORTANT NOTE: You are advised to consult the publisher's version (publisher's PDF) if you wish to cite from it. Please check the document version below.

Document Version
Publisher's PDF, also known as Version of record

[Link to publication in University of Groningen/UMCG research database](#)

Polarized Sphingolipid Transport from the Subapical Compartment: Evidence for Distinct Sphingolipid Domains

Sven C. D. van IJzendoorn and Dick Hoekstra*

Department of Physiological Chemistry, Faculty of Medical Sciences, University of Groningen, 9713 AV Groningen, The Netherlands

In polarized HepG2 cells, the sphingolipids glucosylceramide and sphingomyelin (SM), transported along the reverse transcytotic pathway, are sorted in subapical compartments (SACs), and subsequently targeted to either apical or basolateral plasma membrane domains, respectively. In the present study, evidence is provided that demonstrates that these sphingolipids constitute separate membrane domains at the luminal side of the SAC membrane. Furthermore, as revealed by the use of various modulators of membrane trafficking, such as calmodulin antagonists and dibutyryl-cAMP, it is shown that the fate of these separate sphingolipid domains is regulated by different signals, including those that govern cell polarity development. Thus under conditions that stimulate apical plasma membrane biogenesis, SM is rerouted from a SAC-to-basolateral to a SAC-to-apical pathway. The latter pathway represents the final leg in the transcytotic pathway, followed by the transcytotic pIgR–dIgA protein complex. Interestingly, this pathway is clearly different from the apical recycling pathway followed by glucosylceramide, further indicating that randomization of these pathways, which are both bound for the apical membrane, does not occur. The consequence of the potential coexistence of separate sphingolipid domains within the same compartment in terms of "raft" formation and apical targeting is discussed.

INTRODUCTION

Polarized cells have distinct plasma membrane (PM) domains, which are separated by tight junctions. The apical domain and basolateral domain, thus formed, each displays a specific composition of proteins and lipids. For the establishment and maintenance of such specific compositions, intracellular sorting machineries are operational that secure the correct targeting and delivery of apical and basolateral proteins and lipids. After biosynthesis, sorting of proteins and lipids is thought to occur in the trans-Golgi network, before delivery of the molecules to the PM (Matter and Mellman, 1994; Traub and Kornfeld, 1997). In addition, in the presence of continuous transcellular transport, an auxiliary non-Golgi compartment exists that harbors machineries for sorting and subsequent polarized targeting of apical and basolateral proteins and lipids in the endocytic–transcytotic pathway. Indeed, in the latter pathway sorting of both proteins (Apodaca et al., 1994b; Odorizzi et al., 1996; Futter et al., 1998) and (glyco)sphingolipids (van IJzendoorn et al., 1997; van IJzendoorn and Hoekstra, 1998) occurs in a subapical endosomal compartment, called subapical compartment

(SAC) (van IJzendoorn and Hoekstra, 1999), which is accessible for molecules derived from either PM domain (Hughson and Hopkins, 1990; Apodaca et al., 1994b; Barosso and Sztul, 1994; Knight et al., 1995; Odorizzi et al., 1996; van IJzendoorn and Hoekstra, 1998).

The molecular mechanisms underlying these sorting events are still largely obscure. Yet, instrumental to protein sorting appears to be their clustering, thus giving rise to domains enriched in proteins that are destined for polarized transport. Both coat proteins, such as COP and clathrin (Whitney et al., 1995; Heilker et al., 1996), and adaptins (Pearse and Robinson, 1990) may trigger such a clustering. In fact, clathrin lattices containing adaptins have been identified on the SAC and therefore may well be implicated in the regulation of polarized trafficking (Futter et al., 1998; Okamoto and Jeng, 1998; Okamoto et al., 1998).

Lipids, rather than accompanying proteins in vesicular transport, have been proposed to play an important role in the sorting of apical resident proteins (Simons and Ikonen, 1997). In particular, (glyco)sphingolipids are of interest, because these lipids display a polarized distribution over the basolateral and apical PM domains. Although some important determinants for apical PM-directed sphingolipid transport have been identified in polarized cells (reviewed by Brown and London, 1998; Zegers and Hoekstra, 1998), the

---

* Corresponding author. E-mail address: d.hoekstra@med.rug.nl.

mechanisms that govern polarized sphingolipid trafficking remain as yet unclear. Importantly, the ability of these lipids to self-associate within a membrane (Schroeder *et al.*, 1994), thus giving rise to sphingolipid-enriched domains and serving in turn as a detergent-insoluble matrix for apical-directed proteins, represents a key issue in the sorting concept (Brown and Rose, 1992; Simons and Ikonen, 1997). In this context it should be noted, however, that not only the apically enriched glycosphingolipids, such as glucosylceramide (GlcCer) and Forssman antigen (Nichols *et al.*, 1987; van IJzendoorn *et al.*, 1997; van IJzendoorn and Hoekstra, 1998), are highly detergent insoluble at 4°C, but also sphingomyelin (SM), the ganglioside GM1, and galactosylceramide (GalCer), i.e., basolaterally targeted lipids (van Genderen and van Meer, 1995; van IJzendoorn and Hoekstra, 1998). Evidently, these observations are difficult to reconcile with the notion that sphingolipid domains function exclusively as apical sorting platforms.

Recently, we have demonstrated that the SAC, which constitutes an integral part of the transcytotic pathway in polarized cells (van IJzendoorn and Hoekstra, 1999), represents a major intracellular site in polarized sorting of sphingolipids. The compartment harbors sorting devices for the preferential targeting of fluorescently tagged derivatives of SM and GalCer to the basolateral domain, whereas GlcCer is effectively directed to the apical membrane. Importantly, this sphingolipid trafficking occurs by vesicular means, which implies that the sphingolipids were segregated within the lumenal leaflet of the SAC.

In the present work, we provide evidence for the existence of separate sphingolipid domains at the lumenal side of the SAC membranes in HepG2 cells, as revealed by the differential interference of membrane traffic modulators, such as calmodulin antagonists and dibutyryl cAMP (dbcAMP), with sphingolipid transport from the SAC. Moreover, the trafficking of these domains from the SAC in either apical or basolateral direction can be independently regulated, and depends on cell polarity development.

MATERIALS AND METHODS

Sphingosylphosphorylcholine, 1-β-glucosylsphingosine, TRITC-labeled phalloidin, Hoechst 33250 (bisbenzimide), asialofetuin type I, and cytochalasin D (cytD) were from Sigma (St. Louis, MO). Albumin (from bovine serum, fraction V) was bought from Fluka Chemie (Buchs, Switzerland). 6-[*N*-(7-nitrobenz-2-oxa-1,3-diazol-4-yl)-amino]hexanoic acid (C_6-NBD) was obtained from Molecular Probes (Eugene, OR). DMEM was purchased from Life Technologies (Paisley, Scotland). FCS was bought from BioWhittaker (Verviers, Belgium), and sodium dithionite ($Na_2S_2O_4$) was from Merck (Darmstadt, Germany). Trifluoperazine dimaleate (TFP) was a product from Calbiochem (La Jolla, CA). DbcAMP was obtained from Boehringer Mannheim (Mannheim, Germany). Texas Red-labeled dIgA was kindly provided by Dr. Kenneth Dunn (Indiana University School of Medicine, Indianapolis, IN). All other chemicals were of analytical grade.

Cell Culture

HepG2 cells were cultured as described elsewhere (van IJzendoorn and Hoekstra, 1998). For microscopic or biochemical experiments cells were plated onto glass coverslips or in culture dishes (diameter, 6 cm), respectively. Cells were used three d after plating. At that time the cells had reached an optimal ratio of polarity versus density, in terms of the number of bile canaliculi (BC), formed between two adjacent cells (the membrane boundary of the canaliculus represents the apical membrane) versus the number of cells (van IJzendoorn *et al.*, 1997).

Synthesis of C_6-NBD-labeled Sphingolipids

C_6-NBD-GlcCer and C_6-NBD-SM were synthesized from C_6-NBD and 1-β-glucosylsphingosine and sphingosylphosphorylcholine, respectively, as described elsewhere (Kishimoto, 1975; Babia *et al.*, 1994). The C_6-NBD-lipids were stored at −20°C and routinely checked for purity.

Labeling of Cells with C_6-NBD-Lipids

Cells were washed three times with PBS. C_6-NBD-GlcCer or C_6-NBD-SM was dried under nitrogen, redissolved in absolute ethanol, and injected into HBSS under vigorous vortexing. The final concentration of ethanol did not exceed 0.5% (vol/vol). All lipid analogues were administered to the cells at a concentration of 4 μM.

Transport of C_6-NBD-Lipids from the SAC

To monitor SAC-associated sphingolipid transport, lipid is first accumulated in the SAC, according to a procedure described elsewhere (van IJzendoorn and Hoekstra (1998). A flow chart of the different incubation steps is depicted in Figure 1, including a schematic representation of the cell labeling situation after the corresponding step. First, cells were washed with PBS and incubated with C_6-NBD-SM or -GlcCer at 37°C for 30 min to allow internalization of the lipid analogue from the basolateral surface and transcytosis (Figure 1, step 1) (van IJzendoorn *et al.*, 1997; van IJzendoorn and Hoekstra, 1998; Zegers *et al.*, 1997; Zegers and Hoekstra, 1998). The remaining basolateral pool of lipid analogue was then depleted by a back-exchange procedure (5% [wt/vol] BSA in HBSS, pH 7.4, at 4°C twice for 30 min; Figure 1, step 2). Then the lipid was chased from the apical, bile canalicular PM into the SAC by an incubation at 18°C in back-exchange medium (Figure 1, step 3). The chase was done over a 60-min period and at this time, the vast majority of the lipid analogue was associated with the SAC (Figure 1, step 4; cf. van IJzendoorn and Hoekstra, 1998). Any NBD fluorescence still remaining at the luminal leaflet of the apical PM after the 60-min chase was subsequently abolished by incubating the cells with 30 mM sodium dithionite (diluted from a 1 M stock solution in 1 M Tris buffer, pH 10) at 4°C, a condition that precludes intracellular access of the quencher. After 10 min, the sodium dithionite was then removed by extensive washing (i.e., >10 times) of the cells with ice-cold HBSS. In some experiments, cells were then treated with 20 μM TFP, 100 μM dbcAMP, or 10 μg/ml cytD at 4°C for 30 min (Figure 1, step 4a). Transport of the lipid analogues from the SAC was subsequently monitored by incubation in back-exchange medium at 37°C (Figure 1, step 5). When required, TFP, dbcAMP, and/or cytD were kept present during the transport assay.

To quantitate transport of the lipid analogues to and from the apical, BC membranes, the percentage of NBD-positive BC membranes was determined as described elsewhere (van IJzendoorn *et al.*, 1997; van IJzendoorn and Hoekstra, 1998). Thus, BC were first identified by phase-contrast illumination and then classified as either NBD positive or NBD negative under epifluorescence illumination. Distinct pools of fluorescence were discerned, present in vesicular structures adjacent to BC, which have been defined as SACs (cf. van IJzendoorn and Hoekstra, 1998). Together, BC and SAC thus constitute the bile canalicular, apical pole (BCP) in HepG2 cells. Therefore, within the BCP region the localization of the fluorescent lipid analogues will be defined as being derived from BC, SAC, or both. This also provides a means to describe the movement of the lipid within or out of this region in the cell. Thus, after loading the SAC with lipid analogue and a subsequent incubation as described above (i.e., following step 5 in Figure 1), the direction of movement of the lipid analogue from
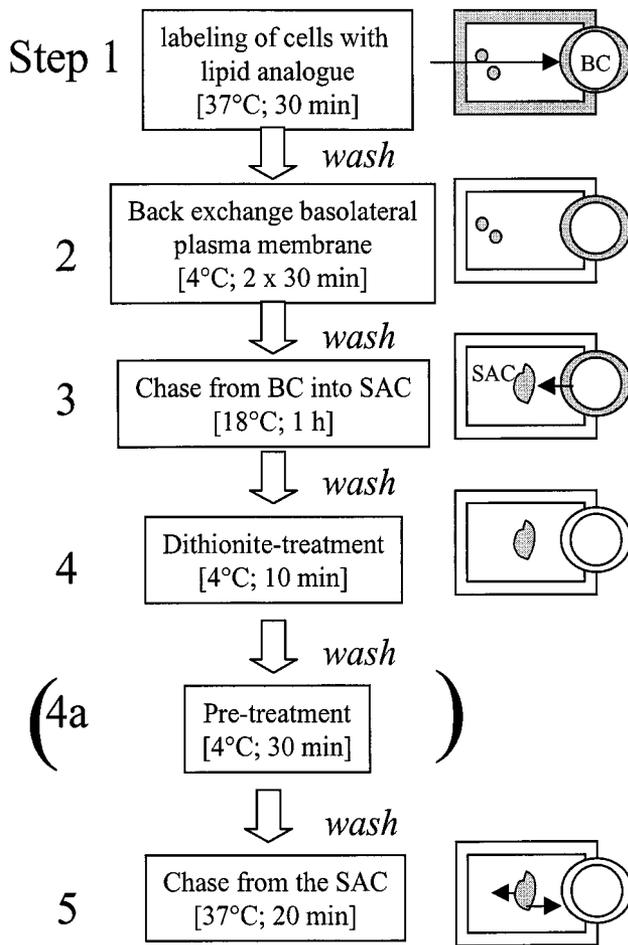
Figure 1. Schematic representation of the various steps of the lipid transport assays. The cell-labeling situation after the corresponding incubation step is depicted at the right. Cells are incubated with C_6-NBD-lipids at 37°C for 30 min, causing labeling of both apical (BC) and basolateral membranes (step 1). Subsequently, the fraction of the fluorescent lipid analogue residing at the basolateral PM is depleted by BSA at 4°C twice for 30 min (step 2). The BC-associated lipid analogue is then chased into SACs at 18°C for 1 h in BSA-containing medium (step 3). The presence of BSA in the medium during this step will prevent reentry of any lipid analogue that might arrive basolaterally during the chase. Next, the NBD-labeled lipid remaining at the BC is quenched by sodium dithionite (step 4). The sodium dithionite is removed by extensive washing (i.e. >10 times) wih ice-cold HBSS. Occasionally, cells were subsequently incubated with TFP, dbcAMP, or both at 4°C for 30 min (step 4a). Transport of the subapically derived lipid analogue can be monitored upon rewarming and incubating the cells at 37°C (step 5).

or within the BCP region is inferred from determining the fraction of NBD-labeled BCP (i.e., label in either the BC or SAC or both) at a given time, relative to that labeled when starting the chase (t = 0). To reproducibly estimate the (re)distribution of the lipid analogue from or within the BCPs, identified in the cell culture, at least 50 BCPs per coverslip were analyzed. Data are expressed as the mean ± SEM of at least three independent experiments, carried out in duplicate.

Basolateral to Apical Transcytosis of Texas Red-labeled dIgA

HepG2 cells that stably express the polymeric immunoglobulin receptor (pIgR; van IJzendoorn and Hoekstra, 1998) were washed, and asialoglycoprotein receptors were saturated with excess asialofetuin at 37°C for 30 min to prevent uptake of dIgA via these receptors (van IJzendoorn and Hoekstra, 1998). Cells were incubated with TxR-dIgA (50 μg/ml) at 4°C for 60 min. Cells were then washed with ice-cold HBSS to remove nonbound TxR-dIgA and further incubated at 18 or 37°C or a combination of both temperatures for various intervals. To investigate the last step of dIgA-pIgR transcytosis, i.e., transfer from the SAC to the apical, bile canalicular PM, asialofetuin-pretreated cells were, after the 4°C binding incubation, incubated with TxR-dIgA at 37°C for 15 min. Then, the temperature was lowered to 18°C, and cells were incubated for an additional 90 min. In this way, most of the transcytosing TxR-dIgA accumulated in the SAC (see Figure 6 and Table 1; cf. van IJzendoorn and Hoekstra, 1998). To examine the effect of TFP on transport of TxR-dIgA from SAC to BC, cells were subsequently treated with HBSS, supplemented with 20 μM TFP at 4°C for 30 min, and incubated in HBSS with TFP at 37°C.

Microscopic Analysis and Image Processing

Cells were examined microscopically using an Olympus (Tokyo, Japan) Provis AX70 fluorescence microscope. Photomicrographs were taken using Ilford (Paramus, NJ) HP5-plus films and subsequently scanned and cropped, using imaging software. All images were converted to tagged information file format before printing on a Fujix (Tokyo, Japan) P3000 printer.

RESULTS

TFP Inhibits Transport of C_6-NBD-SM from SAC to the Basolateral PM

To monitor transport of SM from the SAC, the compartment was loaded with the fluorescent analogue, C_6-NBD-SM, as described in MATERIALS AND METHODS (Figure 1, steps 1–4). The cells were subsequently treated with 20 μM TFP in HBSS at 4°C for 30 min (Figure 1, step 4a). Note that this treatment did not affect the fluorescence distribution associated with the SAC when compared with nontreated cells (our unpublished results, but see van IJzendoorn and Hoekstra, 1998). Transport of C_6-NBD-SM from the SAC was then activated by an incubation at 37°C in back-exchange medium, either in the presence or absence of TFP (Figure 1, step 5). In control cells, C_6-NBD-SM rapidly disappeared from the apical, bile canalicular region, defined as BCP (bile canalicular pole; see MATERIALS AND METHODS) after a 20-min chase (Figure 2A, inset, dotted line). Significant transfer to the apical, bile canalicular PM (BC) was not observed, and the remaining fraction of BCP-associated C_6-NBD-SM was predominantly found in the SAC (Figure 2A, hatched bars). These results are entirely consistent with our previous observations of the SAC, acting as a traffic center for SM distribution in polarized HepG2 cells (van IJzendoorn and Hoekstra, 1998). By contrast, when the cells had been treated with TFP, transport of C_6-NBD-SM from the apical pole was inhibited. Thus, in the presence of the calmodulin antagonist, the extent of BCP labeling in the cell population remained unaltered (Figure 2A, inset, dashed line), whereas the localization of SM was identical to that observed before the chase; i.e., the analogue was almost exclusively associated with the SAC. Importantly, note that
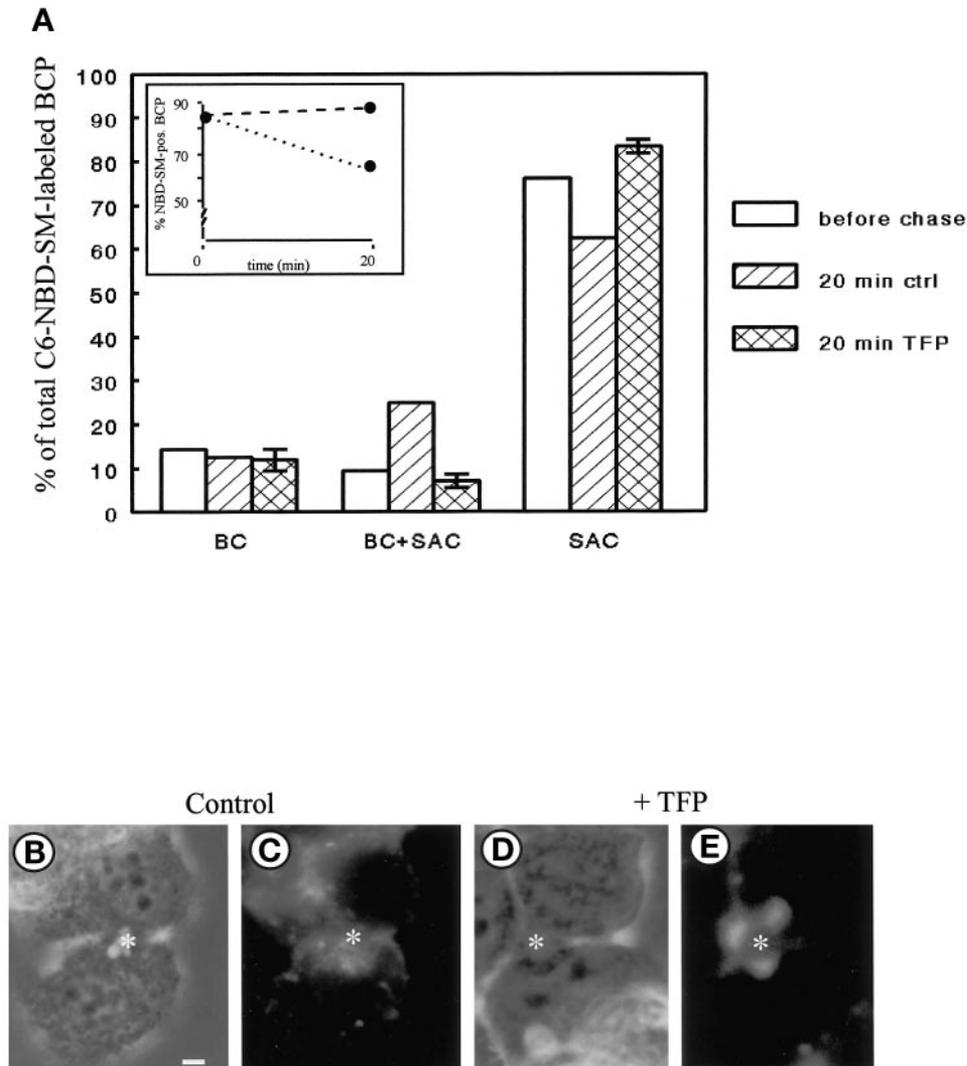
Figure 2. Effect of TFP on transport of C_6-NBD-SM from SAC. C_6-NBD-SM was accumulated into SAC as described in MATERIALS AND METHODS (also cf. van IJzendoorn and Hoekstra, 1998). After abolishing the remaining BC-associated NBD fluorescence with sodium dithionite, cells were treated with HBSS (control) or 20 μM TFP at 4°C for 30 min. Cells were washed and kept in HBSS at 4°C until use (<30 min; t = o, before chase), or alternatively, cells were subsequently warmed to 37°C and further incubated in back-exchange medium for 20 min. Cells were then rapidly cooled and kept on ice until use (<30 min). (A) Semiquantitative analysis of transport from or within the BCP. The percentage of C_6-NBD-SM-labeled BCP (inset; dotted line, control; dashed line, TFP treated) and the distribution of the BCP-associated C_6-NBD-SM (i.e., in BC, SAC, or both) were determined as described in MATERIALS AND METHODS. Data are expressed as mean ± SEM of at least three independent experiments, carried out in duplicate. (B–E) Photomicrographs illustrating the distribution of the lipid analogue in the BCP after a chase from SAC in nontreated (B and C) and TFP-treated (D and E) cells (B and D, phase-contrast to C and E, respectively; asterisk, apical, bile canalicular PM). Bar, 5 μm.

the TFP-mediated inhibition of basolateral transport did not result in a redirection of SM from the SAC to the apical surface (Figure 2, A, cross-hatched bars, and E). Hence, the data show that after arrival of apical PM-derived C_6-NBD-SM in the SAC, TFP inhibits transport of SM from the SAC to the basolateral area of the cells by preventing its exit from this compartment. Similar results were obtained with other calmodulin antagonists such as W7 and calmodazolium (our unpublished results), suggesting that the observed effect reflected a calmodulin-mediated action rather than a TFP-specific effect.

TFP Does Not Affect Apical Recycling of C_6-NBD-GlcCer via SAC

As demonstrated previously (van IJzendoorn and Hoekstra, 1998), the SAC is instrumental in securing the preferential apical distribution of GlcCer in HepG2 cells. To examine the specificity of the TFP block on SM exit from the SAC, we next investigated whether TFP affected transport of C_6-NBD-GlcCer from this compartment. To this end, C_6-NBD-GlcCer was accumulated in the SAC, similarly as described in the previous section for C_6-NBD-SM (also see MATERIALS AND METHODS; Figure 1, steps 1–4). Subsequently, the cells were treated with 20 μM TFP at 4°C for 30 min and incubated for another 20 min at 37°C in back-exchange medium in the presence of the compound (Figure 1, steps 4a and 5). As a control, cells were treated identically but in the absence of TFP. As shown in Figure 3A (white bars), before the chase, the majority of the lipid analogue was in the SAC. After the 20-min chase at 37°C, C_6-NBD-GlcCer remained associated with the BCP (Figure 3A, inset, dotted and dashed lines), irrespective of treatment of the cells with TFP. Interestingly, however, both in the absence and presence of TFP, GlcCer redistributed to the apical surface. Thus, in nontreated cells after the 20-min chase, C_6-NBD-GlcCer was observed in BC alone, BC and SAC, or SAC alone (Figure 3, A, hatched bars, and C), consistent with our previous observation of a preferential apical localization of this analogue

Figure 3. Effect of TFP on transport of C_6-NBD-GlcCer from SAC. C_6-NBD-GlcCer was accumulated into SAC as described in MATERIALS AND METHODS (also cf. van IJzendoorn and Hoekstra, 1998). After abolishing the remaining BC-associated NBD fluorescence with sodium dithionite, cells were treated with HBSS (control) or 20 μM TFP at 4°C for 30 min. Then cells were washed and kept in HBSS at 4°C until use (<30 min; t = 0, before chase), or alternatively, cells were warmed to 37°C and incubated in back-exchange medium for 20 min. Cells were then rapidly cooled and kept on ice until use (<30 min). (A) Semiquantitative analysis of C_6-NBD-GlcCer transport within the BCP. The percentage of C_6-NBD-GlcCer-labeled BCP (inset; dotted line, control; dashed line, TFP treated) and the distribution of the BCP-associated NBD-GlcCer (i.e., BC, SAC, or both) were determined as described in MATERIALS AND METHODS. Data are expressed as mean ± SEM of at least three independent experiments, carried out in duplicate. (B–E) Photomicrographs illustrating the distribution of the lipid analogue in the BCP after a chase from SAC in nontreated (B and C) and TFP-treated (D and E) cells (B and D, phase-contrast to C and E, respectively; asterisk, apical, bile canalicular PM). Bar, 5 μm.
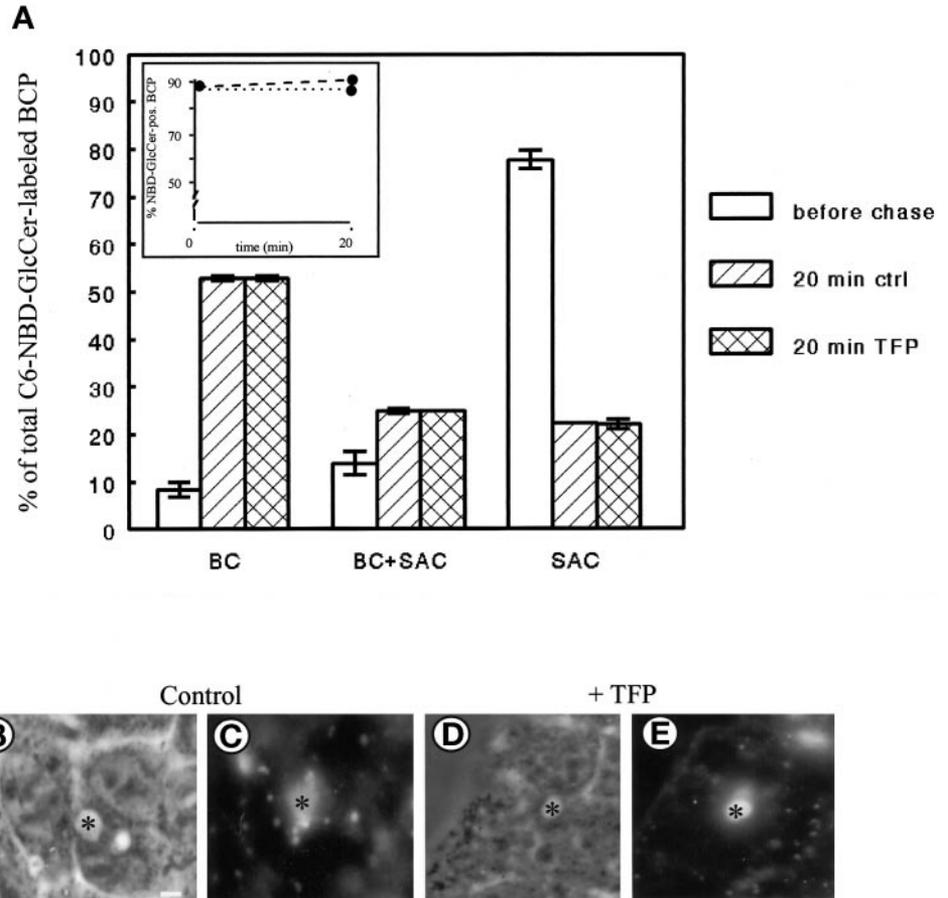
(van IJzendoorn and Hoekstra, 1998). Also in TFP-treated cells, the lipid analogue remained associated with the BCP (Figure 3A, inset, dashed line). Remarkably, however, in this case, GlcCer was redistributed identically as observed in control cells (Figure 3, A, compare cross-hatched bars vs. hatched bars, and E). Hence, the results demonstrate that apical recycling of C_6-NBD-GlcCer via the SAC, in contrast to basolateral directed trafficking of C_6-NBD-SM via the same compartment, is *not* affected by TFP.

TFP Inhibits Apical to Basolateral Transcytosis of C_6-NBD-GlcCer at the Level of SAC

Although the majority of apical PM-derived C_6-NBD-GlcCer is efficiently recycled to the apical surface via the SAC, this lipid analogue does have access to the basolateral PM (van IJzendoorn *et al.*, 1997). Presumably, during each round of apical recycling between the apical membrane and the SAC, part of the lipid analogue "escapes" the recycling route and is transcytosed to the basolateral surface. Indeed, when apical PM-associated C_6-NBD-GlcCer is chased from this membrane domain at 37°C for longer periods in back-exchange medium, thus retrieving any basolateral arriving lipid analogue and preventing its reinternalization, nearly the entire pool of the originally apically located lipid analogue can be depleted. Typically, relative to the control (i.e., in the ab-

sence of back-exchange medium) only 20% of the total BC fraction remains fluorescently labeled over a chase period of 90 min (Figure 4A). To address the issue of the (lipid) specificity of the observed TFP effect on basolateral exit, we next examined whether TFP inhibited apical-to-basolateral transport of C_6-NBD-GlcCer, similarly as observed for C_6-NBD-SM. Hence, cells were labeled with C_6-NBD-GlcCer at 37°C for 30 min. In this way, 70–80% of the BC were labeled with the lipid analogue (Figure 4A, hatched bar). The pool of basolaterally associated lipid analogue was then depleted at 4°C, and during the second step in the back-exchange procedure (see MATERIALS AND METHODS), 20 μM TFP was added for preincubation. The BC-labeled cells were then incubated at 37°C in back-exchange medium supplemented with TFP. Control cells were treated identically but in the absence of TFP. In these cells, the percentage of C_6-NBD-GlcCer-labeled BC decreased from ~75% before the chase to 20% after a 90-min chase (Figure 4A, upper cross-hatched bar), indicating that the lipid analogue was transported out of the apical area to the basolateral membrane. Indeed, the percentage of C_6-NBD-GlcCer-labeled BCP was reduced from 80 to 35% (Figure 4A', solid line). Interestingly, in TFP-treated cells, the percentage of C_6-NBD-GlcCer-labeled BC after the 90-min chase was twice as high as the percentage of BC labeling in nontreated cells (Figure 4A, upper

A

A'

B

C
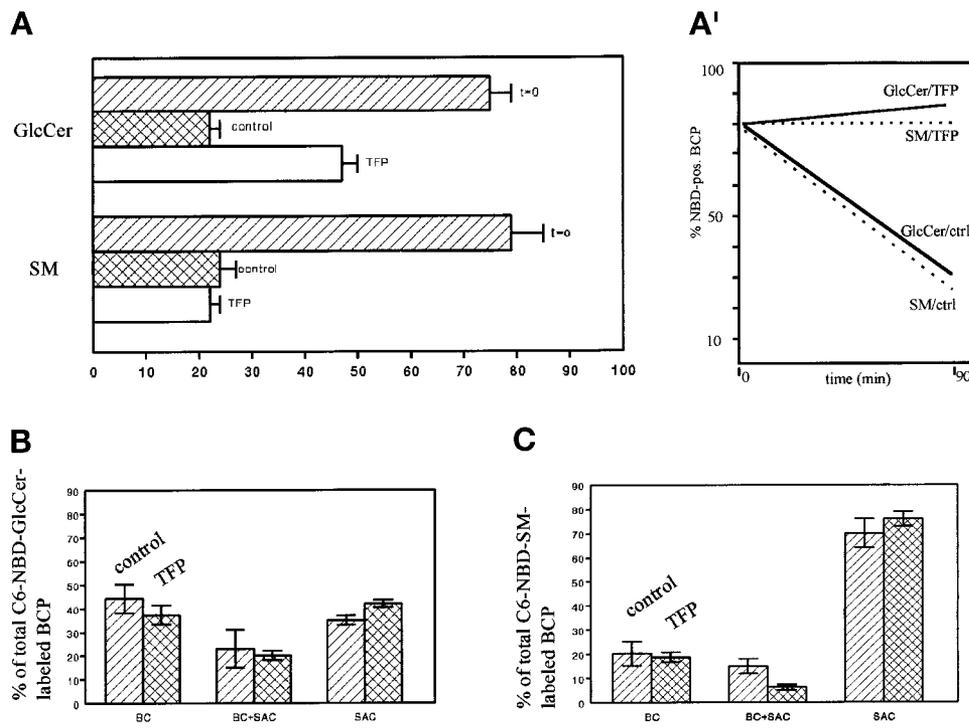
Figure 4. Effect of TFP on apical-to-basolateral transcytosis of fluorescently tagged GlcCer and SM. Cells were labeled with 4 μM C_6-NBD-GlcCer or -SM at 37°C for 30 min. Cells were then incubated in HBSS supplemented with BSA at 4°C twice for 30 min to deplete the basolateral pool of lipid analogue (back-exchange). During the last 30 min of the back exchange procedure 20 μM TFP was added to the cells. As a control, cells were treated identically but in the absence of TFP. Cells were then warmed to 37°C and incubated in back-exchange medium, with or without TFP, for 90 min. (A) Percentage of NBD-SM- or -GlcCer-labeled BC is the 90-min chase. (A') Percentage of NBD-lipid-labeled BCP. Thus, a BCP is NBD positive when labeling of the BC, SAC, or both BC and SAC is observed (see MATERIALS AND METHODS; cf. van IJzendoorn and Hoekstra, 1998). (B and C) Distribution of the (remaining) fraction of BCP-associated C_6-NBD-GlcCer and -SM, respectively.

white bar). This would suggest that apical-to-basolateral transport of the lipid analogue was inhibited, whereas recycling between the SAC and BC was unaffected (see above). Indeed, in TFP-treated cells, the percentage of C_6-NBD-GlcCer-labeled BCP remained constant, maintaining a level of 80–85% during the 90-min incubation period (Figure 4A', solid line). In both control and TFP-treated cells, the remaining fraction of the BCP-associated C_6-NBD-GlcCer was located in BC, SAC, or both (Figure 4B), indicating that the C_6-NBD-GlcCer was remaining at the apical pole and recycled as usual between the apical PM and the SAC.

An interesting lipid species-dependent distinction became apparent when examining similarly the effect of TFP on apical to basolateral transcytosis (originating from BC) of C_6-NBD-SM. In control cells, the percentage of C_6-NBD-SM-labeled BC decreased from ~80% before the chase to ±20% (Figure 4A, lower cross-hatched bar) after a 90-min incubation in back-exchange medium. In TFP-treated cells, a very similar percentage of ~20% of fluorescently labeled BC was observed (Figure 4A, lower white bar). However, in this case the same low percentage of labeled BC did not reflect transport of C_6-NBD-SM out of the apical pole. Thus, in TFP-treated cells, the percentage of C_6-NBD-SM-labeled BCP was still ~80%, whereas in control cells this percentage was ~30% (Figure 4A', dotted lines). Analysis of the distribution of the remaining fraction of BCP-associated C_6-NBD-SM revealed that the majority was located in the SAC alone (Figure 4C). Evidently, and in accordance with the data on transport of the SM analogue from the SAC (Figure 2A, cross-hatched bars), SM became trapped and apparently did not enter the apical recycling pathway instead. It is finally important to note that no metabolism of the lipid analogues

applied occurred during the time span of the experiments (our unpublished results).

Taken together, the data clearly show that TFP inhibits apical-to-basolateral transcytosis of both C_6-NBD-GlcCer and C_6-NBD-SM at the level of the SAC. As a result, basolateral PM-directed transport of both lipid analogues was blocked, whereas apically targeted transport of C_6-NBD-GlcCer was unaffected. Interestingly, TFP does not discriminate between C_6-NBD-SM and -GlcCer during the transport of these analogues from BC to the SAC, nor is sphingolipid transport as such affected. However, when present in the SAC, C_6-NBD-GlcCer and C_6-NBD-SM pools are distinctly recognized by the membrane traffic-modulating compound TFP. Hence, the data strongly suggest that within the SAC membranes C_6-NBD-GlcCer and C_6-NBD-SM are segregated into distinct pools or domains.

If such pools exist, an intriguing possibility would be that lipids, to be retrieved from these pools, might be distinctly regulated. Such a distinct regulation could be reflected by a difference in the traffic pathway by which a particular lipid would reach the same target membrane. To examine this possibility we next studied the effect of dbcAMP and TFP on the trafficking of SM.

DbcAMP Reroutes C_6-NBD-SM from SAC to the Apical PM domain

Previously, we have shown that treatment of the cells with the stable cAMP analogue dbcAMP abolishes apical-to-basolateral transcytosis of C_6-NBD-SM (van IJzendoorn et al., 1997). Instead, analogous to the fate of GlcCer, C_6-NBD-SM remained associated with the apical pole of the cell. It was
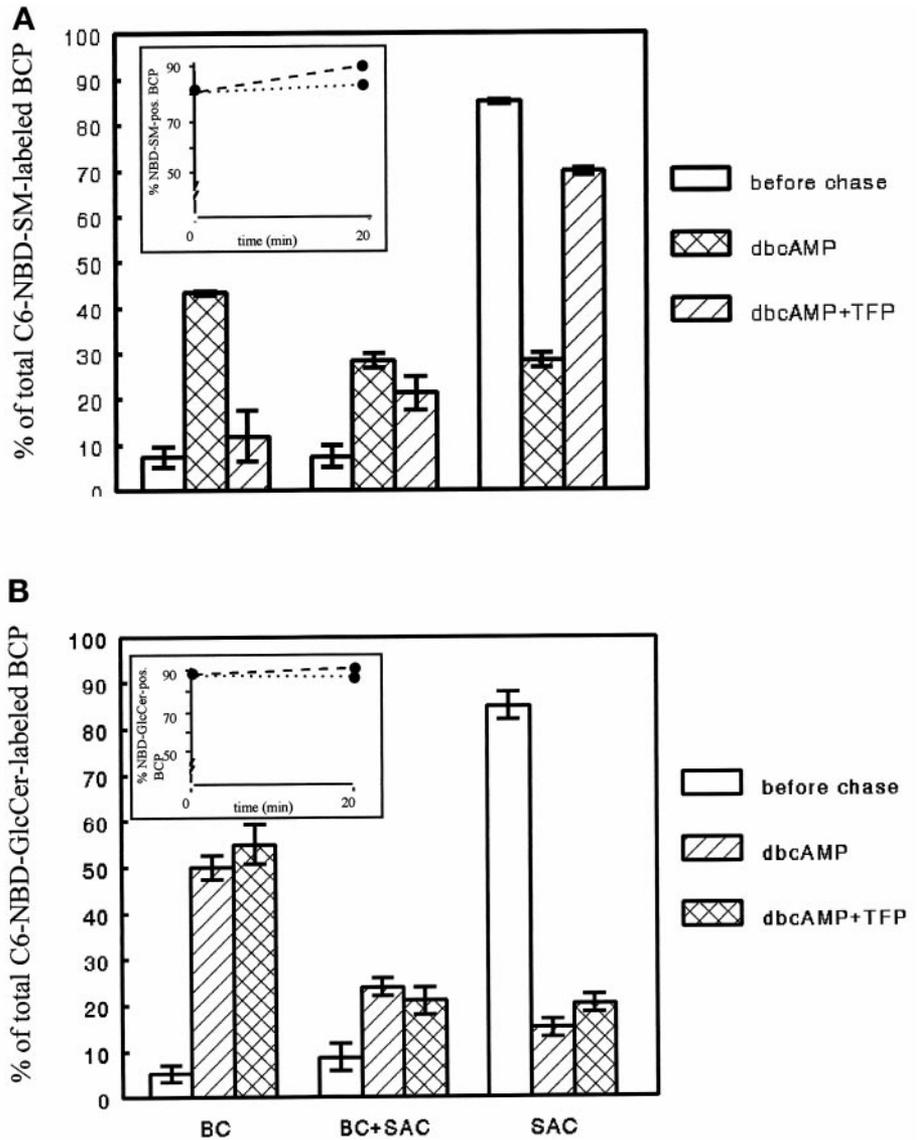
Figure 5. Effect of dbcAMP and a combination of dbcAMP and TFP on transport of C_6-NBD-SM (A) or C_6-NBD-GlcCer (B) from the SAC. C_6-NBD-SM was accumulated into SAC as described in MATERIALS AND METHODS (also cf. van IJzendoorn and Hoekstra, 1998). After abolishing the remaining BC-associated NBD fluorescence with sodium dithionite, cells were treated with HBSS (control), 100 μM dbcAMP, or 100 μM dbcAMP and 20 μM TFP at 4°C for 30 min. Then cells were washed and kept in HBSS at 4°C until use (<30 min; t = 0, before chase) or, alternatively, warmed to 37°C and incubated in back-exchange medium, with either only dbcAMP or both compounds, for 20 min. Cells were then rapidly cooled and kept on ice until use (<30 min). The percentage of C_6-NBD-SM-labeled BCP (inset; dotted line, dbcAMP treated; dashed line, dbcAMP and TFP treated) and the distribution of the BCP-associated NBD-SM (i.e., BC, SAC, or both) were determined as described in MATERIALS AND METHODS. Data are expressed as mean ± SEM of at least two independent experiments carried out in duplicate. (C–F) Photomicrographs illustrating the distribution of the lipid analogue in the BCP after a chase from SAC in dbcAMP-treated (C and D) and dbcAMP- and TFP-treated (E and F) cells (C and E, phase-contrast to D and F, respectively; asterisk, apical, bile canalicular PM). Bar, 5 μm.
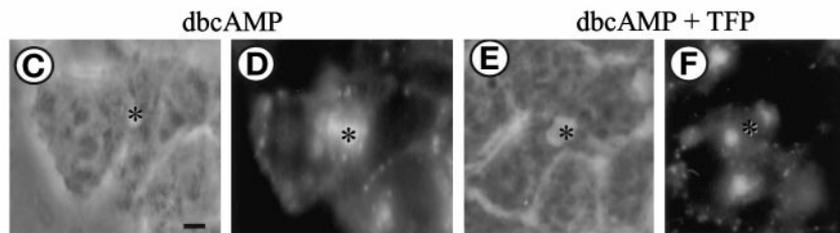
suggested that dbcAMP stimulated apical recycling of C_6-NBD-SM via the SAC, but the site of action was not determined in detail (van IJzendoorn and Hoekstra, 1998). To further examine this issue, the SAC was loaded with apical PM-derived C_6-NBD-SM as described (see MATERIALS AND METHODS; Figure 1, steps 1–4), followed by addition of 100 μM dbcAMP (cf. Figure 1, step 4a). Transport of

SAC-associated C_6-NBD-SM was then activated by shifting the temperature to 37°C and incubating the cells in back-exchange medium, supplemented with dbcAMP (Figure 1, step 5). Whereas in nontreated control cells the percentage of C_6-NBD-SM-labeled BCP decreased from >80 to ~60% after a 20-min incubation (cf. Figure 2A, inset, dotted line), in dbcAMP-treated cells the percentage of C_6-NBD-SM-labeled

BCP remained constant (Figure 5A, inset, dotted line), suggesting that elevated levels of cAMP prevented transport of the lipid analogue out of the apical pole. Moreover, the BCP-associated C_6-NBD-SM did not exclusively label the SAC as observed in nontreated cells (Figure 2A, hatched bars) but was redistributed within the BCP and also labeled BC (Figure 5A, cross-hatched bars). The distribution of C_6-NBD-SM in the BCP is depicted in Figure 5D. Hence, these data indicate that in the presence of dbcAMP C_6-NBD-SM recycled between the SAC and the apical PM domain, similarly as observed for C_6-NBD-GlcCer in nontreated cells (Figure 3A, hatched bars). Taken together, the data show that dbcAMP reroutes SAC-associated C_6-NBD-SM from the basolateral to the apical PM. Hence, the question can now be raised of whether SM participates in the same recycling pathway as that observed for GlcCer. We therefore examined the effect of TFP on the apically directed flow of SM and GlcCer, exiting from the SAC.

TFP Inhibits SAC-to-Apical Transport of C_6-NBD-SM but Not -GlcCer in DbcAMP-treated Cells

To examine the effect of TFP on dbcAMP-induced transport of the C_6-NBD-lipids from the SAC to the apical PM, 20 μM TFP was included during those incubation steps at which dbcAMP was present (i.e., Figure 1, steps 4a and 5; see MATERIALS AND METHODS). As shown in Figure 5A (inset, dashed line), the presence of TFP did not affect the pool of C_6-NBD-SM that remained associated with the apical pole (BCP) of the cell in the presence of dbcAMP alone (Figure 5A, inset, dotted line). However, in contrast to the cells that had been treated with dbcAMP alone, which show a distribution of the SM analogue over both BC and the SAC, TFP- and dbcAMP-treated cells display a distribution in which the vast majority of C_6-NBD-SM in the BCP remained in the SAC alone. Only a relatively small fraction of the lipid analogue had been transported from SAC to BC (Figure 5A, hatched bars). The BCP distribution of C_6-NBD-SM in TFP-treated cells, as revealed by fluorescence microscopy, is shown in Figure 5F. Interestingly, apical recycling of C_6-NBD-GlcCer via the SAC was unaffected by TFP (Figure 5B) in both control and dbcAMP-treated cells. These data strongly suggest, therefore, that in dbcAMP-treated cells C_6-NBD-GlcCer and -SM remained in distinct pools or subdomains. Apparently, dbcAMP does not interfere with the segregation of the lipid analogues in the SAC. Furthermore, the discriminating effect of TFP on SAC-to-BC transport of C_6-NBD-SM and -GlcCer implies that at least two independent pathways from the SAC to BC exist. By monitoring the trafficking of the polymeric Ig receptor–IgA complex, a well-established transcytotic marker, the nature of these different pathways was further investigated.

TFP Inhibits the Final Step of Basolateral to Apical Transcytosis of TxR-dIgA, Its Delivery from SAC to the Apical Surface

In a previous study, we have shown that basolaterally endocytosed receptor-bound dIgA (pIgR–dIgA) passes through the SAC before delivery at the apical surface of HepG2 cells, whereas the complex accumulates in the SAC when the temperature is lowered to 18°C (van IJzendoorn and Hoekstra, 1998). To investigate whether TFP affected
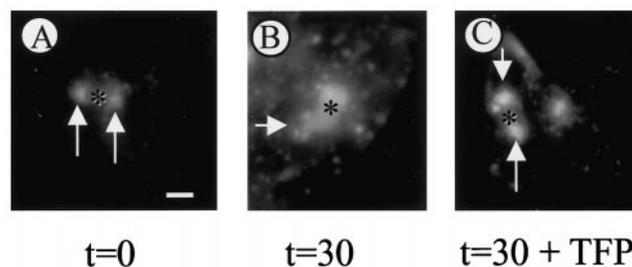
Figure 6. Effect of TFP on SAC-to-BC transport of TxR-labeled dIgA. Cells that stably express the polymeric immunoglobulin receptor (van IJzendoorn and Hoekstra, 1998) were washed and incubated with excess asialofetuin to saturate asialoglycoprotein receptors. Subsequently, cells were incubated with 50 μg/ml TxR-dIgA at 4°C for 1 h. After rinsing the cells to remove nonbound ligand, cells were warmed to 37°C and incubated for 15 min to allow internalization and partial transcytosis. Then, cells were rapidly cooled to 18°C and further incubated for 90 min. (A) Basolateral PM-derived TxR-dIgA has accumulated in SAC (arrows). (B) After a subsequent incubation at 37°C, TxR-labeled both SAC and BC, indicative of transport to BC. However, in the presence of TFP, SAC-to-BC transport of TxR-IgA was severely inhibited. Most of the fluorescently labeled dIgA was still in SAC alone (arrows) with little if any TxR-dIgA transported to BC. A semiquantitative analysis is presented in Table 1. Asterisks, apical, bile canalicular PM. Bar, 10 μm.

transport of pIgR–dIgA from SAC to the apical, bile canalicular PM domain, HepG2 cells that stably express the pIgR were washed, pretreated with excess asialofetuin to saturate asialoglycoprotein receptors, and incubated with 50 μg/ml Texas Red-labeled dIgA (TxR-dIgA) at 4°C for 60 min. Then, nonbound TxR-dIgA was removed by rinsing the cells with ice-cold HBSS, and the cells incubated in HBSS at 37°C to allow internalization. After 15 min, the cells were cooled to 18°C and incubated for another 90 min. This incubation procedure caused the vast majority of the transcytosing TxR-dIgA to accumulate in the SAC, whereas the amount reaching the apical PM domain was essentially negligible (Figure 6A and Table 1). Cells were then treated with 20 μM TFP or HBSS at 4°C for 30 min and subsequently incubated in HBSS with or without TFP at 37°C for 30 min. Whereas in nontreated cells, TxR-dIgA was readily transported from the SAC to BC (Figure 6B), apical delivery of TxR-dIgA from the SAC was inhibited by TFP treatment (Figure 6C). Indeed, the percentage of TxR-dIgA-positive BC in TFP-treated cells was significantly decreased when compared with HBSS-treated cells (Table 1). Hence, the data show that TFP inhibits trafficking of TxR-dIgA from the SAC to BC, suggesting that pIgR-dIgA and C_6-NBD-SM are transported along the same pathway from the SAC to BC in dbcAMP-treated cells. Apparently, this pathway differs from that followed by the GlcCer analogue, traveling between the SAC and BC, as its trafficking is unaffected by TFP.

DbcAMP Causes Hyperpolarization of HepG2 Cells, Which is Abolished by TFP

While analyzing sphingolipid trafficking in dbcAMP-treated cells, it was readily observed that the number of apical PM domains, BC, as well as their size was increased. To define

Table 1. Accumulation of transcytosing TxR-labeled IgA in SAC and subsequent delivery to BC; effect of TFP

	BC	BC + SAC	SAC
15' 37°C → 90' 18°C	0± 0	4± 2	96± 2
15' 37°C → 90' 18°C → buffer → 30' 37°C	19.1± 1.7	62.4± 7.4	18.6± 5.6
15' 37°C → 90' 18°C → TFP → 30' 37°C (+TFP)	2.5± 1.5	22.5± 2.5	75± 5

Cells were washed and incubated with excess asialofetuin to saturate asialoglycoprotein receptors (see MATERIALS AND METHODS). Subsequently, the cells were incubated with 50 μg/ml TxR-IgA at 4°C for 1 h. After rinsing the cells to remove nonbound ligand, cells were warmed to 37°C and incubated for 15 min (15[1]) to allow internalization and partial transcytosis. Then, the cells were rapidly cooled to 18°C and further incubated for 90 min. As shown in the first row, after this incubation scheme ~96% of the label located in the BCP was due to the exclusive labeling of SAC. Subsequently, the cells were incubated in HBSS (control) or HBSS supplemented with 20 μM TFP at 4°C for 30 min and for an additional 30 min at 37°C in the presence or absence of TFP. In buffer-treated cells, a clear shift of TxR-IgA labeling from SAC to BC was seen to have occurred, leaving only 18% of the ligand in SAC alone (second row). In TFP-treated cells, this shift was effectively inhibited, as judged by the presence of the vast majority of BCP-associated label in SAC. Only a relatively minor fraction of the TxR-IgA was transported from SAC to BC (third row). Data are expressed as mean ± SEM of at least four independent experiments.

Table 2. Effect of dbcAMP and/or TFP or a sequential incubation of a combination of both on polarity of the cells

	Ratio [BC/100 cells]
Control	10.2 ± 1.5
DbcAMP	21.3 ± 0.5
TFP	9.5 ± 1.0
DbcAMP + TFP	10.8 ± 0.5
DbcAMP → TFP	19.2 ± 1.0
TFP → dbcAMP	9.7 ± 1.5

For incubation schemes see text. After the incubations, the cells were fixed and permeabilized with −20°C ethanol for 10 s, rehydrated in HBSS, and incubated with TRITC-labeled phalloidin and Hoechst to determine the ratio [BC/100 cells] (cf. Zegers *et al.*, 1997). Data are presented as mean ± SEM of two or three independent experiments.

the parameters that affected the degree of cell polarity and to appreciate the relevance of distinct pathways involved, the following experimental conditions were examined. First, the cells were treated with 100 μM dbcAMP at 4°C for 30 min and subsequently at 37°C for 30 min. Alternatively, 1) cells were treated with 20 μM TFP; 2) cells were simultaneously treated with TFP and dbcAMP; 3) cells were first incubated with dbcAMP for 30 min at 4 and 37°C and subsequently incubated with TFP at 37°C for 30 min; 4) cells were first incubated with TFP for 30 min at 4 and 37°C and subsequently incubated with dbcAMP at 37°C for 30 min; or finally, 5) cells were treated with buffer. After fixation and permeabilization in −20°C ethanol for 10 s and rehydration in HBSS, the cells were subsequently double stained with Hoechst and TRITC-labeled phalloidin and the ratio [BC/100 cells] was determined as described in MATERIALS AND METHODS. The results are presented in Table 2. DbcAMP treatment caused an increase of the ratio [BC/100 cells] and, thus, enhanced cell polarity by ~200% when compared with buffer-treated cells. However, when the cells had simultaneously been treated with TFP, this increase in polarity was abolished. Importantly, TFP alone did not affect the polarity of the cells. Because the calmodulin antagonist inhibited apical-directed transport from the SAC in dbcAMP-treated cells (see Figure 6) and did not cause depolarization as such, the results thus suggest that dbcAMP-induced hyperpolarization is due to a stimulation of apical directed transport via the SAC. Indeed, when cells were treated with TFP, before dbcAMP, no change in the ratio [BC/100 cells] was observed, suggesting that the dbcAMP-induced hyperpolarization is closely correlated to an en-

hanced membrane flow, typified by the pathway followed by C_6-NBD-SM and pIgR–dIgA from the SAC. Totally in agreement with this, TFP was unable to counteract the hyperpolarized state of the cells when administered after db-cAMP.

Transport of C_6-NBD-Lipids from SAC does not Depend on an Intact Actin Filament Network

The exiting of C_6-NBD-SM and -GlcCer from the SAC, either in basolateral or apical direction in dbcAMP-treated cells, is vesicle mediated (van IJzendoorn and Hoekstra, 1998). It is possible therefore that the calmodulin antagonist inhibits the formation of C_6-NBD-lipid-containing vesicles (see DISCUSSION). Calmodulin functions as a light chain for myosin (Geli *et al.*, 1998), which is an actin- and ATP-dependent molecular motor. Both myosin (Müsch *et al.*, 1997) and actin (Gottlieb *et al.*, 1993) have been suggested to be important factors in vesicle formation. Hence, calmodulin might play a role in the regulation of cytoskeleton rearrangements and, thus, vesicle formation. Interestingly, myosin II has been suggested to interfere with the transport of secretory vesicles across the cortical actin meshwork at a late, postmicrotubular stage (Ayscough *et al.*, 1997). Moreover, recycling of PM components from the perinuclear recycling endosome, the proposed SAC equivalent in nonpolarized cells (Zacchi *et al.*, 1998; van IJzendoorn and Hoekstra, 1999), is regulated by ADP ribosylating factor-6 GTPase (D'Souza-Schorey *et al.*, 1998), which, in turn, is also implicated in modeling the cortical actin cytoskeleton (Song *et al.*, 1998). To test whether transport of the lipid analogues from the SAC required intact actin filaments, the SAC was loaded with either lipid as described in MATERIALS AND METHODS (cf. Figure 1, steps 1–4). Subsequently, cells were incubated with the actin filament-disrupting drug cytD at 4°C for 30 min (cf. Figure 1, step 4a). Then, the cells were rewarmed to 37°C and incubated for an additional 20 min in the presence of cytD (Figure 1, step 5). Although cytD effectively disrupted actin filaments as evidenced by staining with fluorescently labeled phalloidin (cf. Zegers *et al.*, 1998, their Figure 1D), no effect on SAC-to-basolateral or SAC-to-apical transport of C_6-NBD-SM and -GlcCer, respectively, was observed (Figure 7, A and B; compare with Figures 2A and 3A, respec-

A

B
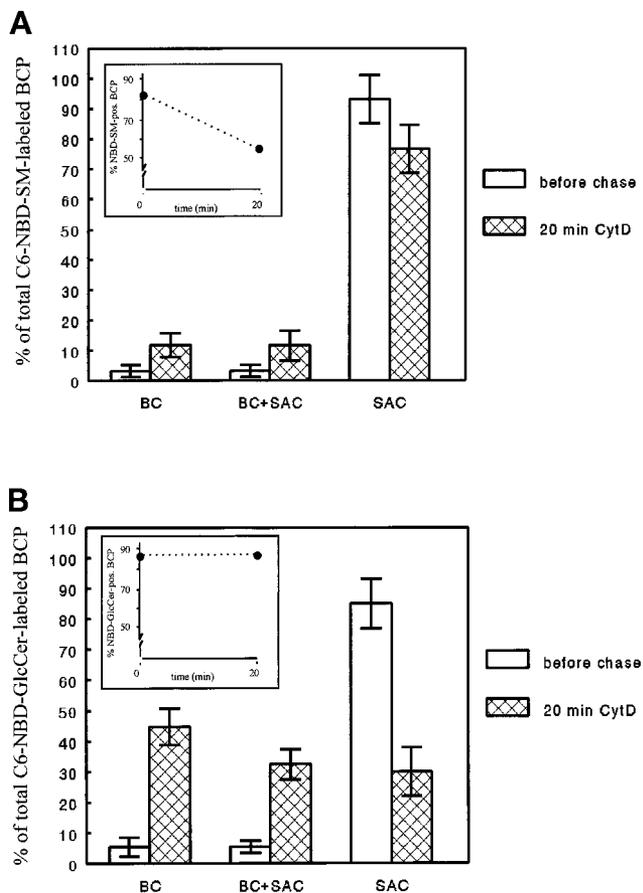
Figure 7. Effect of the actin filament disrupting agent cytD on transport of C_6-NBD-SM (A) and -GlcCer (B) from SAC. C_6-NBD-lipid was accumulated into SAC as described in MATERIALS AND METHODS. After abolishing the remaining BC-associated NBD fluorescence with sodium dithionite, cells were treated with 10 μg/ml cytD at 4°C for 30 min. Then they were washed and kept in HBSS at 4°C until use (<30 min; t = 0, before chase) or, alternatively, warmed to 37°C and incubated in back-exchange medium in the presence of cytD for 20 min. Cells were then rapidly cooled and kept on ice until use (<30 min). The percentage of NBD-lipid-labeled BCP (inset) and the distribution of the BCP-associated NBD-lipid (i.e., BC, SAC, or both) before (white bars) and after the chase from SAC (cross-hatched bars) was determined as described in MATERIALS AND METHODS. Data are expressed as mean ± SEM of at least two independent experiments carried out in duplicate.

tively). Hence, it is unlikely that TFP inhibited C_6-NBD-SM-containing vesicle formation from SAC by perturbing actin filament organization.

DISCUSSION

C_6-NBD-SM and -GlcCer Are in Distinct Domains in the SAC in Polarized HepG2 Cells

In the present work, we have obtained novel insight into the molecular sorting of distinct sphingolipids in the reverse transcytotic pathway in polarized HepG2 cells. In particular,

the direct involvement and the significance of the previously identified subapical compartment, SAC, as a major sorting compartment in generating cell polarity, was further highlighted. Thus, neither apical endocytosis nor subsequent transport to the SAC of either SM or GlcCer was affected by the calmodulin antagonist TFP. However, after having reached this compartment, the antagonist strongly interfered with the subsequent fate of the sphingolipids, revealing at least three different membrane flow pathways originating from the SAC. As shown previously (van IJzendoorn and Hoekstra, 1998), in the reverse transcytotic pathway, sorting occurs in this compartment, SM being directed to the basolateral membrane, whereas GlcCer returns from the SAC to the apical PM. In the presence of TFP, the latter pathway still occurred (Figure 3). However, the antagonist selectively and strongly inhibited the exit of C_6-NBD-SM from the SAC (Figure 2). Interestingly, being barred from exiting in a basolateral-directed pathway, a rerouting of SM into the apical pathway, as marked by GlcCer flow, did not occur. In contrast to its inertness in the GlcCer recycling pathway (see Figure 4), TFP inhibited the exiting of the SAC-associated GlcCer that, in time, escapes from the apical route and instead is targeted to the basolateral membrane (van IJzendoorn et al., 1997). Similarly, in polarized Madin–Darby canine kidney (MDCK) cells, calmodulin antagonists similarly have been shown to inhibit the basolateral recycling of transferrin (Apodaca et al., 1994a), thus impeding trafficking between the basolateral membrane and SACs that are closely related to or inherently part of SAC (Odorizzi et al., 1996; Futter et al., 1998; van IJzendoorn and Hoekstra, 1999). Interestingly, an apical membrane-directed flow of C_6-NBD-SM from the SAC could be activated upon treatment of the cells with dbcAMP. Remarkably, in contrast to the recycling pathway of the GlcCer analogue, the dbcAMP-controlled apical pathway of SM could be completely blocked by TFP treatment. Hence, TFP prevents the entry of both SAC-associated SM and GlcCer into a basolateral route, whereas it distinguishes between SAC-to-apical transport of SM and GlcCer. It is evident therefore, that the apical membrane-directed pathways of both lipids, exiting from SAC, are different. Specifically, because TFP also inhibited transport of basolaterally endocytosed dIgA–pIgR from the SAC to BC, the evidence supports the view that in dbcAMP-activated cells, SM is transported to the apical membrane via the same TFP-sensitive basolateral-to-apical transcytotic pathway.

Apparently, treatment of the cells with TFP and/or db-cAMP did not cause randomization of the distinct sphingolipid pools in the SAC membranes. Thus, whereas the transport of GlcCer in the apical recycling pathway continued in TFP-treated cells, SM accumulated in the SAC rather than being directed into an alternative traffic pathway. This emphasizes the specificity of the process, presumably reflecting an interference with domain-specific signals, as part of a trafficking machinery. The inability of SM to exit from the SAC suggests that the mechanism of TFP relates to an interference with an early step in the transport pathway from SAC, rather than with sorting or polarized targeting, such as docking and fusion of transport vesicles. Consistent with this is the finding that in MDCK cells, TFP inhibited basolateral-to-apical transcytosis of dIgA–pIgR, similarly as observed in this study, resulting in an intracellular accumula-

tion of the complex in large early endosomal compartments, whereas no enhanced basolateral recycling was observed (Apodaca *et al.*, 1994a). Moreover, Enrich *et al.* (1996) identified pIgR as the major calmodulin-binding protein in a rat liver endosomal fraction enriched in recycling receptors and presumably SAC membranes, whereas Chapin *et al.* (1996) showed that although calmodulin binds to the autonomous basolateral targeting signal of pIgR, neither is it necessary nor does it interfere with basolateral targeting of pIgR. The mechanism by which the calmodulin antagonist would interfere with vesiculation from the SAC remains to be determined but appears not to be mediated via perturbation of actin filaments (Figure 7). Consistent with this is the finding that transport of pIgR–dIgA from the SAC in MDCK cells was similarly unaffected after treatment with cytD (Maples *et al.*, 1997).

Taken together, at least three different membrane flow pathways that originate from SAC are distinguished, mediating transport to either the basolateral or the apical membrane, while given the different responsiveness to the various exogenous treatments as described, each route is likely controlled by a different traffic-regulating machinery. In part, this regulation may involve the molecular organization of relevant compounds into separate (membrane) domains, which must be located in the inner leaflets of the SAC membranes. Such a localization is dictated by topological requirements, because transport of both lipid analogues to and from the SAC is vesicle mediated; i.e., lipid translocation and monomeric lipid transfer have been excluded (van IJzendoorn and Hoekstra, 1998). It is finally of interest to note that the fate of such distinct domains can be subject to control, related to specific biological demands, in this particular case a change of cell polarity.

Distinctly Regulated Sphingolipid Trafficking Pathways Exit from SAC: A Correlation with Apical PM Biogenesis

Activation of different steps in the adenylate cyclase–cAMP–protein kinase A signal transduction cascade has been reported to stimulate transport to the apical PM domain in polarized cells (Hansen and Casanova, 1994; Mostov and Cardone, 1995; Zegers and Hoekstra, 1997). In agreement with this notion, treatment of HepG2 cells with dbcAMP enhances apical PM-directed transport of C_6-NBD-SM and -GlcCer via a protein kinase A-mediated mechanism, and causes a concomitant hyperpolarization of the cells (this study; cf. Zegers and Hoekstra, 1997). The present data demonstrate that the traffic machinery in the SAC acts as a target site for the cAMP analogue. Because hyperpolarization was completely abolished upon simultaneous treatment of the cells with dbcAMP and TFP, a close correlation between the transport pathway from the SAC to BC, as marked by the trafficking of C_6-NBD-SM in cAMP-treated cells and the biogenesis of apical PM, is suggested. Furthermore, because dbcAMP was unable to cause hyperpolarization in TFP-pretreated cells, whereas TFP did not reverse dbcAMP-induced hyperpolarization (Table 2), it is apparent that transport along this pathway from the SAC to BC precedes apical PM biogenesis. Indeed, elsewhere we have demonstrated that dbcAMP treatment mobilizes sphingolipid trafficking from an intracellular pool, rather than stimulating endocytosis at the basolateral membrane or the biosynthesis of sphingolipids (Zegers and Hoekstra, 1997). Hence, our data

point to the SAC as a likely candidate for dbcAMP-induced, i.e., signal-mediated, stimulation of apical transcytosis and the importance of this pathway, as marked by the TFP-sensitive SM/dIgA–pIgR route, in polarity development.

Distinct Sphingolipid Domains: Implications for Polarized Transport

Sphingolipid domains, referred to as rafts, have been proposed to play a pivotal role in the transport of apical proteins (Brown and Rose 1992; Simons and Ikonen, 1997). Typically, these domains are identified by their isolation as Triton X-100-insoluble fractions (at 4°C), enriched in distinct proteins, cholesterol, and sphingolipids such as GlcCer and SM (Brown and Rose 1992). The present observations raise some intriguing questions concerning the composition and specificity of raft-mediated trafficking. First of all, although acyl chain saturation has been mechanistically related to raft formation (Ahmed *et al.*, 1997; Simons and Ikonen, 1997; Brown and London, 1998; Zegers and Hoekstra, 1998), the hydrophobic parts of the fluorescent analogues are identical, implying that their sorting into distinct domains must be largely driven by head group specificity. The next question that arises is whether and to what extent these lipids, being located in separate domains, each can participate in the formation of such rafts. Could they possibly participate in the formation of distinct rafts, each directed to a different, i.e., apical or basolateral, target membrane? In this context, it is not unlikely that the distribution of rafts (and their functioning) may be more ubiquitous than revealed thus far (Brown and London, 1998; Mayor *et al.*, 1998; this study). Evidently, further work is obviously required, but these issues may have important consequences with respect to the exclusiveness of raft-specific (i.e., apical) targeting and claims concerning their composition when isolated by detergent extraction. In this respect it is important to emphasize that both C_6-NBD-SM and C_6-NBD-GalCer are targeted from the SAC to the basolateral membrane (van IJzendoorn and Hoekstra, 1998), although we have not yet determined whether these analogues are randomized within the same domain. It is apparent though, that when the membrane flow pathway of SM is reversed from basolateral to an apical direction upon treatment of the cells with dbcAMP, the SM and GlcCer domains do maintain their specific identity.

Interestingly, in the hepatic cell system, several apical GPI-linked proteins have been reported to reach this membrane in an indirect pathway, i.e., a route that leads via the basolateral membrane (Schell *et al.*, 1992; Ihrke *et al.*, 1998). Because newly synthesized SM and GlcCer also appear to travel through SAC before reaching their final destination (van IJzendoorn, Mostov, and Hoekstra, unpublished observations), the present data might therefore suggest that different raft-like domains with different destinations are in fact available for trafficking. It could also explain why several nonapical proteins are found in the detergent-insoluble fraction (Weimbs *et al.*, 1997). Hence, the present observations indicate the potential existence of multiple sphingolipid-enriched domains in the same membrane fraction, which cannot be distinguished as separate entities in detergent extracts. It is apparent that a detailed analysis of these domains, closely related to sorting and targeting governed by as yet unknown mechanisms, paves the way for identifying novel concepts in membrane cell biology in general and polarized trafficking in particular.

ACKNOWLEDGMENTS

REFERENCES

Ahmed, S.N., Brown, D.A., and London, E. (1997). On the origin of sphingolipid/cholesterol-rich detergent-insoluble cell membranes: physiological concentrations of cholesterol and sphingolipid induce formation of a detergent-insoluble, liquid-ordered lipid phase in model membranes. Biochemistry *36*, 10944–10953.

Apodaca, G., Enrich, C., and Mostov, K.E. (1994a). The calmodulin antagonist, W-13, alters transcytosis, recycling, and the morphology of the endocytic pathway in Madin-Darby canine kidney cells. J. Biol. Chem. *269*, 19005–19013.

Apodaca, G., Katz, G.A., and Mostov, K.E. (1994b). Receptor-mediated transcytosis of IgA in MDCK cells is via apical recycling endosomes. J. Cell Biol. *125*, 67–86.

Ayscough, K.R., Stryker, J., Pokala, N., Sanders, M., Crews, P., and Drubin, D.G. (1997). High rates of actin filament turnover in budding yeast and roles for actin in establishment and maintenance of cell polarity revealed using the actin inhibitor latrunculin-A. J. Cell Biol. *137*, 399–416.

Babia, T., Kok, J.W., and Hoekstra, D. (1994). The use of fluorescent lipid analogues to study endocytosis of glycosphingolipids. In: Receptor Research Methods, ed. B. Greenstein, London: Harwood Academic Publishing, 155–174.

Barosso, M., and Sztul, E.S. (1994). Basolateral to apical transcytosis in polarized cells is indirect and involves BFA and trimeric G protein sensitive passage through the apical endosome. J. Cell Biol. *124*, 83–100.

Brown, D.A., and London, E. (1998). Functions of lipid rafts in biological membranes. Annu. Rev. Cell Dev. Biol. *14*, 111–136.

Brown, D.A., and Rose, J.K. (1992). Sorting of GPI-anchored proteins to glycolipid-enriched membrane subdomains during transport to the apical surface. Cell *68*, 533–544.

Chapin, S.J., Enrich, C., Aroeti, B., Havel, R.J., and Mostov, K.E. (1996). Calmodulin binds to the basolateral targeting signal of the polymeric immunoglobulin receptor. J. Biol. Chem. *271*, 1336–1342.

D'Souza-Schorey, C., van Donselaar, E., Hsu, V.W., Yang, C., Stahl, P.D., and Peters, P.J. (1998). ARF6 targets recycling vesicles to the plasma membrane: insights from an ultrastructural investigation. J. Cell Biol. *140*, 603–616.

Enrich, C., Jackle, S., and Havel, R.J. (1996). The polymeric immunoglobulin receptor is the major calmodulin-binding protein in an endosome fraction from rat liver enriched in recycling receptors. Hepatology *24*, 226–232.

Futter, C.E., Gibson, A., Allchin, E.H., Maxwell, S., Ruddock, L.J., Odorizzi, G., Domingo, D., Trowbridge, I.S., and Hopkins, C.R. (1998). In polarized MDCK cells basolateral vesicles arise from clathrin-gamma-adaptin-coated domains on endosomal tubules. J. Cell Biol. *141*, 611–623.

Geli, M.I., Wesp, A., and Riezman, H. (1998). Distinct functions of calmodulin are required for the uptake step of receptor-mediated endocytosis in yeast: the type I myosin Myo5p is one of the calmodulin targets. EMBO J. *17*, 635–647.

Gottlieb, T.A., Ivanov, I.E., Adesnik, M., and Sabatini, D.D. (1993). Actin microfilaments play a critical role in endocytosis at the apical but not the basolateral surface of polarized epithelial cells. J. Cell Biol. *120*, 695–710.

Hansen, S.H., and Casanova, J.E. (1994). Gs alpha stimulates transcytosis and apical secretion in MDCK cells through cAMP and protein kinase A. J. Cell Biol. *126*, 677–687.

Heilker, R., Manning-Krieg, U., Zuber, J.F., and Spiess, M. (1996). In vitro binding of clathrin adaptors to sorting signals correlates with endocytosis and basolateral sorting. EMBO J. *15*, 2893–2899.

Hughson, E.J., and Hopkins, C.R. (1990). Endocytic pathways in polarized Caco-2 cells: identification of an endosomal compartment accessible from both apical and basolateral surfaces. J. Cell Biol. *110*, 337–348.

Ihrke, G., Martin, G.V., Shanks, M.R., Schrader, M., Schroer, T.A., and Hubbard, A.L. (1998). Apical plasma membrane proteins and endolyn-78 travel through a subapical compartment in polarized WIF-B hepatocytes. J. Cell Biol. *141*, 115–133.

Kishimoto, Y. (1975). A facile synthesis of ceramides. Chem. Phys. Lipids *15*, 33–36.

Knight, A., Hughson, E., Hopkins, C.R., and Cutler, D.F. (1995). Membrane protein trafficking through the common apical endosome compartment of polarized Caco-2 cells. Mol. Biol. Cell *6*, 597–610.

Maples, C.J., Ruiz, W.G., and Apodaca, G. (1997). Both microtubules and actin filaments are required for efficient postendocytotic traffic of the polymeric immunoglobulin receptor in polarized Madin-Darby canine kidney cells. J. Biol. Chem. *27*, 6741–6751.

Matter, K., and Mellman, I. (1994). Mechanisms of cell polarity: sorting and transport in epithelial cells. Curr. Opin. Cell Biol. *6*, 545–554.

Mayor, S., Sabharanjak, S., and Maxfield, F.R. (1998). Cholesterol-dependent retention of GPI-anchored proteins in endosomes. EMBO J. *17*, 4626–4638.

Mostov, K.E., and Cardone, M.H. (1995). Regulation of protein traffic in polarized epithelial cells. Bioessays *17*, 129–138.

Müsch, A., Cohen, D., and Rodriguez-Boulan, E. (1997). Myosin II is involved in the production of constitutive transport vesicles from the TGN. J. Cell Biol. *138*, 291–306.

Nichols, G.E., Shiraishi, T., Allietta, M., Tillack, T.W., and Young, W.W., Jr. (1987). Polarity of the Forssman glycolipid in MDCK epithelial cells. Biochim. Biophys. Acta *930*, 154–166.

Odorizzi, G., Pearse, A., Domingo, D., Trowbridge, I.S., and Hopkins, C.R. (1996). Apical and basolateral endosomes of MDCK cells are interconnected and contain a polarized sorting mechanism. J. Cell Biol. *135*, 139–152.

Okamoto, C.T., Karam, S.M., Jeng, Y.Y, Forte, J.G., and Goldenring, J.R. (1998). Identification of clathrin and clathrin adaptors on tubulovesicles of gastric acid secretory (oxyntic) cells. Am. J. Physiol. *274*, C1017–C1029.

Okamoto, C.T., and Jeng, Y.Y. (1998). An immunologically distinct β-adaptin on tubulovesicles of gastric oxyntic cells. Am. J. Physiol. *275*, C1323–C1329.

Pearse, B.M., and Robinson, M.S. (1990). Clathrin, adaptors, and sorting. Annu. Rev. Cell Biol. *6*, 151–171.

Schell, M.J., Maurice, M., Stieger, B., and Hubbard, A.L. (1992). 5'Nucleotidase is sorted to the apical domain of hepatocytes via an indirect route. J. Cell Biol. *119*, 1173–1182.

Schroeder, R., London, E., and Brown, D. (1994). Interactions between saturated acyl chains confer detergent resistance on lipids and glycosylphosphatidylinositol (GPI)-anchored proteins: GPI-anchored proteins in liposomes and cells show similar behavior. Proc. Natl. Acad. Sci. USA *91*, 12130–12134.

Simons, K., and Ikonen, E. (1997). Functional rafts in cell membranes. Nature *38*, 569–572.

Song, J., Khachikian, Z., Radhakrishna, H., and Donaldson, J.G. (1998). Localization of endogenous ARF6 to sites of cortical actin rearrangement and involvement of ARF6 in cell spreading. J. Cell Sci. *111*, 2257–2267.

Traub, L.M., and Kornfeld, S. (1997). The trans-Golgi network: a late secretory sorting station. Curr. Opin. Cell Biol. *9*, 527–533.

van Genderen, I., and van Meer, G. (1995). Differential targeting of glucosylceramide and galactosylceramide analogs after synthesis but not during transcytosis in Madin-Darby canine kidney cells. J. Cell Biol. *131*, 645–654.

van IJzendoorn, S.C.D., and Hoekstra, D. (1998). (Glyco)sphingolipids are sorted in subapical compartments in HepG2 cells: a role for nonGolgi-related intracellular sites in the polarized distribution of (Glyco)sphingolipids. J. Cell Biol. *142*, 683–696.

van IJzendoorn, S.C.D., and Hoekstra, D. (1999). The subapical compartment: a novel sorting center? Trends Cell Biol. *9*, 144–149.

van IJzendoorn, S.C.D., Zegers, M.M.P., Kok, J.W., and Hoekstra, D. (1997). Segregation of glucosylceramide and sphingomyelin occurs in the apical to basolateral transcytotic route in HepG2 cells. J. Cell Biol. *137*, 347–357.

Weimbs, T., Low, S.H., Chapin, S.J., and Mostov, K.E. (1997). Apical targeting in polarized epithelial cells: there's more afloat than rafts. Trends Cell Biol. *7*, 393–399.

Whitney, J.A., Gomez, M., Sheff, D., Kreis, T.E., and Mellman, I. (1995). Cytoplasmic coat proteins involved in endosome function. Cell *83*, 703–713.

Zacchi, P., Stenmark, H., Parton, R.G., Orioli, D., Lim, F., Giner, A., Mellman, I., Zerial, M., and Murphy, C. (1998). Rab17 regulates membrane trafficking through apical recycling endosomes in polarized epithelial cells. J. Cell Biol. *140*, 1039–1053.

Zegers, M.M.P., and Hoekstra, D. (1997). Sphingolipid transport to the apical plasma membrane domain in human hepatoma cells is controlled by PKC and PKA activity: a correlation with cell polarity in HepG2 cells. J. Cell Biol. *138*, 307–321.

Zegers, M.M.P., and Hoekstra, D. (1998). Mechanisms and functional features of polarized membrane traffic in epithelial and hepatic cells. Biochem. J. *336*, 257–269.

Zegers, M.M.P., Zaal, K.J.M., van IJzendoorn, S.C.D., Klappe, K., and Hoekstra, D. (1998). Actin filaments and microtubules are involved in different membrane traffic pathways that transport sphingolipids to the apical surface of polarized HepG2 cells. Mol. Biol. Cell *9*, 1939–1949.